08

Endohedral small metallofullerenes as a basis for the formation of heterostructures

© *A.R. El Zanin, S.V. Boroznin, I.V. Zaporotskova, N.P. Boroznina*

Volgograd State University,
400062 Volgograd, Russia
e-mail: nmtb-201_341523@volsu.ru

Received December 19, 2023
Revised December 19, 2023
Accepted December 19, 2023

The study of heterostructures with specific physico-chemical properties useful for the needs of nanoelectronics, microsystems engineering and other branches of nanotechnology is important and relevant. A separate class of chemical compounds in a number of such materials are structures that include various modifications of carbon nanoobjects. One of the most popular nanostructures are fullerenes, the study of which was started at the end of the XX century and continues to the present day. Now the attention of researchers is focused on fullerenes with a small diameter, the composition of which is described by the formulas C_{20}, C_{24}, C_{28}. It is known that the presence of a cavity in fullerenes makes it possible to intercalate them with atoms and even small molecules. Endohedral complexes of fullerenes with alkali (Li, Na, K) and transition (Ti, Zn) metals were considered. The study was carried out using quantum chemical modeling methods within the framework of density functional theory in the B3LYP variant using the basic sets 6-311++G(d,p) and cc-pVDZ. We obtained optimized structures of endohedral fullerenes $M@C_{20,24,28}$ ($M = Li, Na, K$), as well as $Zn@C_{28}$ and $Ti@C_{28}$, and calculated the values of the energy gap of each complex. Based on this, it was concluded that it is possible to form heterostructures based on some of these materials.

Keywords: endohedral metallofullerenes, heterostructures, charge distribution, energy gap.

DOI: 10.21883/0000000000

Introduction

Traditional solid-state electronics currently faces serious challenges in further miniaturization of devices due to the so-called short-channel effects, high leakage current and contact resistance [1]. Therefore, the high contact resistance in the metal–semiconductor system, due to the high potential barrier — the Schottky barrier, — significantly reduces the energy efficiency and performance of devices that have such contacts [2]. For these reasons, carbon nanomaterials and heterostructures based on them are attracting increasing attention of researchers, which make it possible to implement devices on fundamentally new physical bases [3]. Their application for the manufacture of photodetectors [4,5], diodes and transistors [6,7] is justified.

Fullerenes are one of the most well-known and widely studied nanomaterials. They are convex polyhedra consisting of pentagons and hexagons, at the vertices of which carbon atoms are located in the state of sp^2-hybridization. The presence of a cavity inside such structures makes it possible to control their physico-chemical properties by introducing various atoms and molecules. Such complexes are called endohedral [8,9]. Their molecular formula, in the case of a single interstitial atom, is written as M@Cn, where M is an interstitial atom, n is the number of atoms in the carbon cage. It is noted that fullerenes modified by metal atoms can find their applications in electronics and optoelectronic devices as components of photovoltaic cells, transistors, photodetectors, in medicine for targeted drug delivery, diagnostics (for example, for contrast in MRI) [10–20].

The possibility of forming thin films based on fullerenes and controlling their conductive properties by intercalation with metal atoms suggests their potential application as a basis for heterostructures. Heterostructures with both organic [7,21] and inorganic components [22–24], obtained on the basis of well-studied fullerenes C_{60} and with C_{70}, were studied. It can be assumed that such intercalated systems can be based on relatively little-studied fullerenes with fewer than 60 atoms, i.e. the so-called small fullerenes [25,26]. The complexity of their experimental production is associated with their low stability. For fullerenes, the so-called isolated pentagon rule holds, according to which the most stable structures are those in which the pentagons do not have adjacent edges. For fullerenes with fewer than 60 carbon atoms, this rule is not feasible, which may explain the low stability of such structures. Nevertheless, endohedral complexes with metals often turn out to be more stable than pure fullerenes [27,28], which, together with their unique properties [29], suggests their possible use for practical applications in the future.

The optical properties of pure small fullerenes today attract a lot of attention from researchers [30–34]. The intercalation with metal atoms significantly expands the prospects of the considered class of materials for optical applications. It is known that there is a relationship between

the refractive index of a material and the band gap [35,36]. It is possible to assume that the introduction of metal atoms into the fullerene cavity will result in a change of the band gap of such an endohedral structure and, accordingly, targeted control of the refractive index of the medium is possible, which may be useful for the design of photonic crystals. However, to date, no comprehensive studies of small-diameter endohedral fullerenes with introduced atoms have been conducted, which suggests the need for systematic studies of this class of nanomaterials.

The regularities of the impact of metal atoms (Li, Na, K, Ti, Zn) embedded in the cavity of small fullerenes C_{20}, C_{24}, C_{28} on the geometric and electron-energy structure of endohedral systems are studied in this paper. These metals were selected on the basis of previous studies of the metallization of nanoobjects, where the embedding made it possible to change the electronic properties [37]. The study was carried out within the framework of density functional theory using the potential B3LYP [38] and the basis sets 6-311++G(d,p) and cc-pVDZ.

1. Materials and methods

The studied objects were fullerenes $C_{20}(I_h)$, $C_{24}(D_{6d})$, $C_{28}(D_2)$ and their complexes with alkali metal atoms Li, Na, K embedded in the cavity, as well as fullerene $C_{28}(D_2)$ intercalated with transition metal atoms Ti and Zn. The accepted designations of point symmetry groups [39,40] were indicated in brackets. At the first stage of the study, the geometry of the initial fullerenes was optimized, and then the selected metal atom was placed in the center of the fullerene cavity, and repeated optimization was performed.

Calculations were performed within the framework of the density functional theory in the B3LYP approximation. Density functional theory is currently one of the most reliable and proven methods for quantum chemical calculations [41–44]. It is based on the Kohn–Sham equation. Let's define the type of functional for the average energy:

$$E[n] = \langle \Psi[n] | \left(\hat{T} + \hat{U} + \hat{V}_{ext}\right) | \Psi[n] \rangle$$

$$= T + U + V_{ext} = T_S + V_H V_{ext} + (T - T_S + U - V_H).$$

The last term in this expression is responsible for the contribution of the exchange-correlation energy:

$$V_{XC} = (T - T_S + U - V_H).$$

This expression includes four terms, the pairwise difference of which in total gives the specified energy value. The first difference is between the kinetic energies of interacting and free particles, and the second difference is between the energies of the Coulomb interaction and Hartree.

For greater certainty, it is possible to rewrite the Kohn–Sham functional with an indication of the functional dependence of the terms before proceeding to specific calculations:

$$E_{KS}[n] = T_S[n] + V_H[n] + V_{ext}[n] + V_{XC}[n].$$

We will set the appropriate ratios to perform variation:

$$\frac{\delta E_{KS}}{\delta \Psi_{i\sigma}(r)} = \frac{\delta T_S}{\delta \Psi_{i\sigma}}$$

$$+ \left[\frac{\delta V_H}{\delta n(r)} + \frac{\delta V_{ext}}{\delta n(r)} + \frac{\delta V_{XC}}{\delta n_r}\right] \frac{\delta n(r)}{\delta \Psi_{i\sigma}(r)} = 0,$$

$$\frac{\delta T_S}{\delta \Psi_{i\sigma}(r)} = -\frac{1}{2}\nabla^2 \Psi_{i\sigma}(r).$$

The introduction of the Lagrange multiplier (denoted below $\varepsilon_{i\sigma}$) sets the normalization condition. It is possible to write the Kohn –Sham equation taking into account the above:

$$-\frac{1}{2}\nabla^2 \Psi_{i\sigma}(r) + v_{KS}(r)\Psi_{i\sigma}(r) = \varepsilon_{i\sigma}\Psi_{i\sigma}(r).$$

This equation coincides in appearance with the single-particle Schrodinger equation, which describes the behavior of a particle in a self-consistent potential, given by the expression

$$v_{kS}(r) = v_{ext}(r) + v_H(r) + v_{XC}(r),$$

$$v_{ext}(r) = \int dr' \frac{n(r')}{|r - r'|},$$

$$v_{XC}(r) = \frac{\delta V_{XC}}{\delta n(r)},$$

$$n(r) = \sum_{i\sigma} |\Psi_{i\sigma}(r)|^2.$$

The basic set 6-311++G(d,p) was used to model complexes with alkali metals. This basic set has proven itself well for the study of small fullerenes; a number of publications can be noted in which researchers also used it for similar tasks [45,46]. Calculations of C_{28} fullerene complexes with Ti and Zn atoms were performed using the cc-pVDZ basic set.

Such parameters as the average bond length d_{C-C} between carbon atoms of fullerenes and the average distance from the carbon atoms of the cell to the interstitial metal atom 1 were calculated to describe the geometry changes associated with the intercalation of fullerenes by metals.

The charge distribution was analyzed based on the results of calculations of the values of atomic partial charges according to Mulliken [47,48]. The value of the dipole moment μ was also taken into account. Determining this value will allow judging the charge distribution in endohedral fullerene and the possibility of its use as a component of heterostructures. The matter is that endohedral fullerenes can exhibit ferroelectric properties [8]; the spontaneous polarization that occurs in them contributes to the separation of electrons and holes generated by photons of incident light. The greater the dipole moment, the more intense this process is, which increases the efficiency of heterostructures used as photovoltaic elements [25]. Such an effect makes it possible to increase the productivity

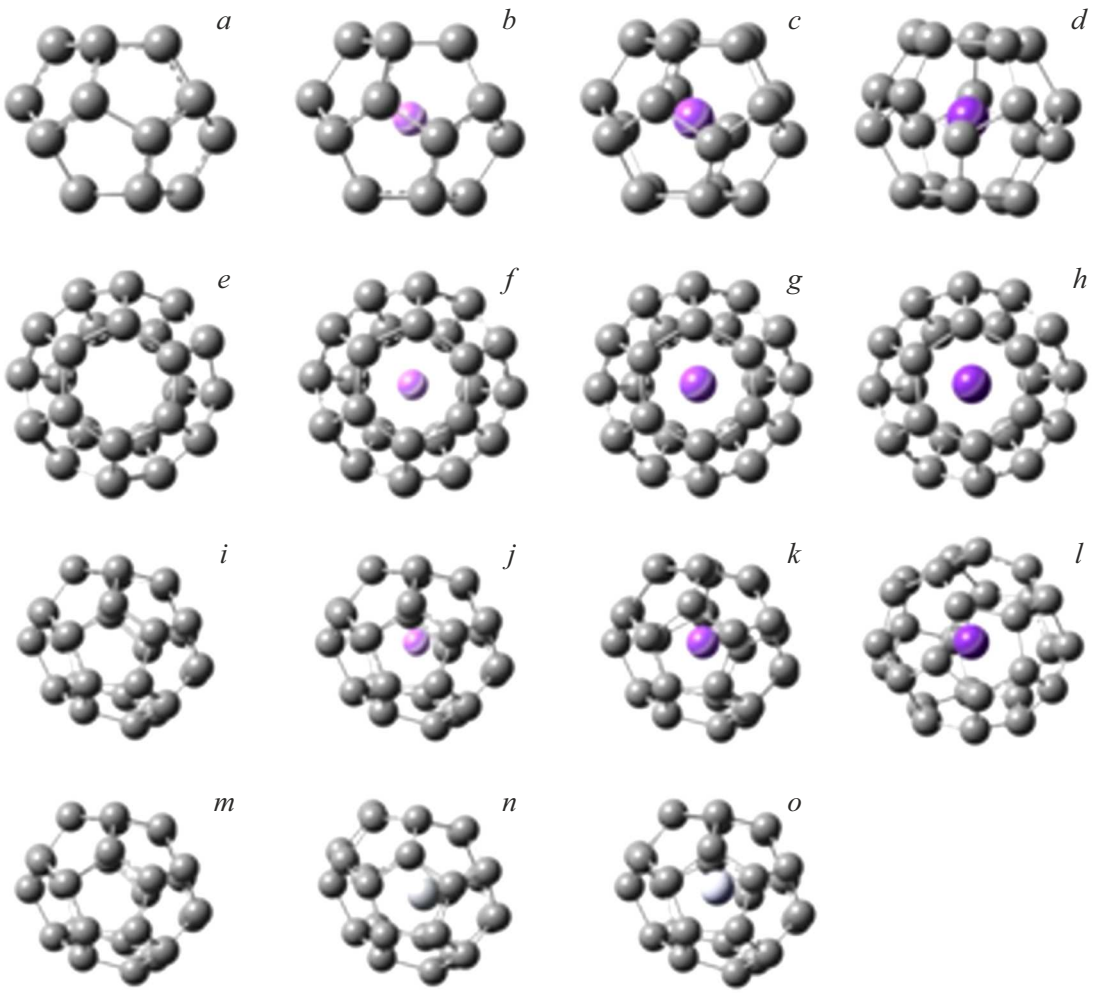

Figure 1. Optimized structures of fullerenes C_{20} (*a*), Li@C_{20} (*b*), Na@C_{20} (*c*), K@C_{20} (*d*), C_{24} (*e*), Li@C_{24} (*f*), Na@C_{24} (*g*), K@C_{24} (*h*), C_{28} (*i*), Li@C_{28} (*j*), Na@C_{28} (*k*), K@C_{28} (*l*), C_{28}^{*} (*m*), Ti@C_{28} (*n*), Zn@C_{28} (*o*).

of the operation of heterostructures, which makes layered nanostructures based on endohedral fullerenes a more promising material.

The band gap ΔE_g was chosen as the main value determining the electron-energy properties of fullerenes and their complexes with metals, the value of which was calculated as the difference between the energy of the lower vacant molecular orbital E_{LUMO} and the energy of the upper filled molecular orbital E_{HOMO}:

$$\Delta E_g = E_{\mathrm{LUMO}} - E_{\mathrm{HOMO}}.$$

The program GaussSum [49] was used to plot the density of states function.

The resulting optimized structures are shown in Fig. 1.

2. Results and discussion

It was found in the result of performed study that intercalation of small fullerenes by metal atoms in all cases causes an increase of the average bond length of carbon–carbon by an average of 1.8%. A trend can be distinguished for alkali metals: the average length of bond C–C increases with an increase of the ordinal number, and the average distance from carbon atoms to a metal atom is 1.

The embedding of the Li atom in fullerene C_{20} causes an increase of the average bond length in the carbon cage compared to the initial structure by 1.3%, the embedding of the Na atom increases the average bond length by 2.7%, and the embedding of the K atom increases of the average bond length by 5.6%. However, already in the next considered representative of the class such as fullerene C_{24} the effect of metal intercalation is less significant. Therefore, the embedding of the Li atom results in an increase of the average bond length by 0.5%, Na — by 1.3%, K — by 3.0%. The effect of intercalation on geometric parameters remains reduced with a further increase of the number of carbon atoms in fullerene. The embedding of the Li atom in fullerene C_{28} results in an increase of the average bond length of carbon–carbon by 0.4%, the introduction of Na increases the average bond length by 0.8%, the

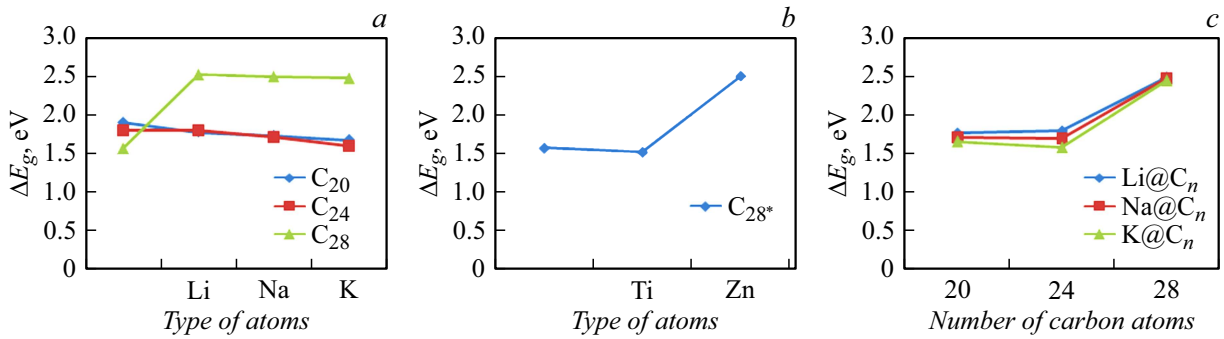

Figure 2. The dependence of the band gap width on the type of interstitial atom (*a* — for alkali metals, *b* — for transition metals), on the number of carbon atoms in fullerene with the same type of interstitial metal atom (*c*). * indicates the use of the cc-pVDZ basic set; the 6-311G(d,p) basic set was used in other cases.

embedding of K increases the average bond length by 1.9%. A decrease of the impact of the intercalating atom on the average distance from carbon atoms to a metal atom with an increase of the number of carbon atoms in the framework of the structure. For instance, the average distance from carbon atoms to the interstitial atom Na is by 1.5% greater than the distance to the Li atom for fullerene C_{20}, it is by 0.8% greater for fullerene C_{24} and by 0.5% greater for fullerene C_{28}. The situation is similar for complexes with an interstitial potassium atom. Taken together, all this indicates that the embedding of alkali metal atoms into the cavity of fullerenes increases their volume, and the greater the ordinal number of the embedded alkali metal atom and, accordingly, the radius of the atom, the more the volume of fullerene increases. But the degree of this impact on the geometry of the structure is lower for fullerenes containing a larger number of carbon atoms, than for fullerenes with a smaller number of carbon atoms.

Let's consider the impact of the embedding of atoms of selected transition metals on the geometry of fullerene C_{28}. The average bond length of carbon–carbon increases by 1.2% compared with the initial fullerene in case of embedding of Ti, it increases by 1% in case of embedding of Zn. It should be noted that the embedding of the Ti atom has a stronger impact on the geometric characteristics of the fullerene C_{28} than the embedding of the Zn atom.

Metal atoms act as electron density donors, the charge from them passes to the carbon atoms of the fullerene cell. Let's denote the charge on the embedded metal atom Q_{Me}. In the case of fullerene C_{20}, this quantity assumes the values of 1.8, 2.5 and 6.4 for complexes with Li, Na and K, respectively. It should be noted that the electron density is distributed evenly in all three cases, as evidenced by the rather close values of the negative charge on the carbon atoms. The average charge on carbon atoms in $Li@C_{20}$ is -0.09, it is equal to -0.13 in $Na@C_{20}$, it is equal to -0.32 in $K@C_{20}$. The values of the dipole moments of the considered complexes are extremely small, the maximum value of 0.0038 D is observed in the K-containing complex, which indicates a low degree of polarization of the clusters. These data are provided to confirm and clarify the above thesis about the uniformity of charge distribution on carbon atoms. The value of Q_{Me} also increases in case of fullerene C_{24}, with an increase of the ordinal number of the metal. However, we observe here an uneven distribution of the electron density. This is supported by relatively high values of dipole moments (on the order of 1.0000 D) for all complexes C_{24}. Interestingly, the dipole moment is greater in the case of $Na@C_{24}$, than in the case of $K@C_{24}$. The reason is that the lowest charge value in the first structure is -0.32, the lowest charge value in the second structure is -0.29. However, the average charge value on carbon atoms is lower for the complex with K and is -0.19, and the average charge value on carbon atoms complex with Na is -0.17. Therefore, the electron density shifts from the K atom to the fullerene cell to a greater extent, but more evenly, while it shifts more unevenly from the Na atom, which is why a comparatively stronger polarization is observed. The charge value Q_{Me} is maximal in fullerene C_{28} in case of intercalation by the Na atom. The magnitude of the dipole moment is of the greatest importance for the complex with Li, and it decreases with an increase of the ordinal number of the metal. Therefore, the uniformity of the electron density distribution increases in the series $Li@C_{28} < Na@C_{28} < K@C_{28}$, while the electron density shifts to the greatest extent from the Na atom to the carbon atoms of the cell in comparison with by other atoms considered.

When introducing the atom Zn into the fullerene cell C_{28} we observe a more pronounced shift of the electron density from the metal atom to the carbon atoms of the cell than in the case of the Ti atom. However, a large polarization is observed in the endohedral fullerene $Ti@C_{28}$, the value of the dipole moment of this compound is the largest compared to all the structures considered in the work and is comparable to the dipole moment $Cr@C_{28}$, given in Ref. [25]. The difference between the maximum and minimum charge values on carbon atoms in $Ti@C_{28}$ is greater than in $Zn@C_{28}$, which once again confirms the conclusion about the degree of polarization.

Let us consider the change of the band gap in small fullerenes as a result of the impact of one of two factors:

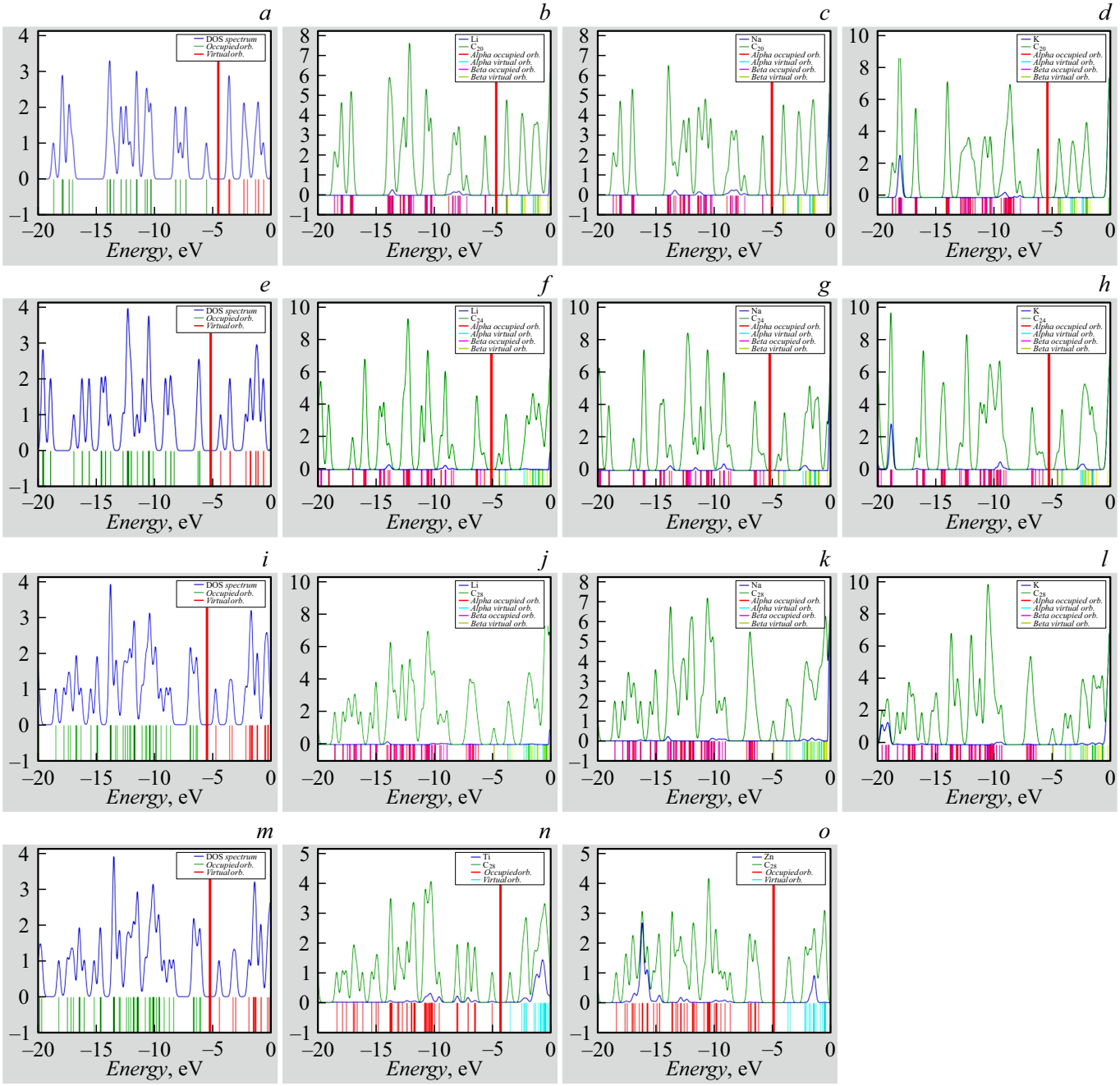

Figure 3. Density of states functions for fullerenes C_{20} (*a*), Li@C_{20} (*b*), Na@C_{20} (*c*), K@C_{20} (*d*), C_{24} (*e*), Li@C_{24} (*f*), Na@C_{24} (*g*), K@C_{24} (*h*), C_{28} (*i*), Li@C_{28} (*j*), Na@C_{28} (*k*), K@C_{28} (*l*), C_{28}^{*} (*m*), Ti@C_{28} (*n*), Zn@C_{28} (*o*). The density of states function in the images (*a*), (*e*), (*i*), (*m*) has a blue color, green color in the single-electron spectrum indicates the electron energy levels of the valence band, red color indicates the electron energy levels of the conduction band. Green color on (*b*)–(*d*), (*f*)–(*h*), (*j*)–(*l*), (*n*), (*o*) indicates the density of states function, blue color indicates the contributions of metal atoms. The bold red line on all images except (*j*)–(*l*) indicates the Fermi level.

the introduction of atoms of various metals with a constant number of carbon atoms in the fullerene frame and a change of the number of carbon atoms in the fullerene cell with the same type of embedded atom.

The dependences of the band gap width on the type of embedded atom are shown in Fig. 2, *a, b*. The effect of the introduction of alkali metal atoms on the electronic structure of fullerene C_{20} is enhanced in the series Li<Na<K, namely, the band gap in this series decreases from 1.784 for lithium to 1.682 for potassium, therefore, we observe the best conductive properties in endohedral fullerene K@C_{20}. The intercalation of fullerene C_{24} by the Li atom slightly increases the band gap. The band gap decreases with the embedding of Na and K atoms. A rather atypical

Geometric, energetic and electron-conducting properties of small fullerenes and their endohedral complexes with metals

Metal	$d_{C\text{-}C}$, Å	l, Å	Q_{Me}	μ, D	E_{LUMO}, eV	E_{HOMO}, eV	ΔE_g, eV
C_{20}	1.451	–	–	0.0001	–3.624	–5.531	1.907
Li@C_{20}	1.470	2.057	1.85	0.0002	–3.829	–5.613	1.784
Na@C_{20}	1.490	2.088	2.53	0.0004	–4.079	–5.814	1.735
K@C_{20}	1.532	2.147	6.39	0.0038	–4.510	–6.192	1.682
C_{24}	1.455	–	–	0.0009	–4.315	–6.123	1.808
Li@C_{24}	1.462	2.260	0.77	0.9958	–3.929	–5.741	1.812
Na@C_{24}	1.474	2.279	4.13	1.0033	–4.035	–5.753	1.718
K@C_{24}	1.498	2.316	4.50	0.9292	–4.230	–5.835	1.605
C_{28}	1.448	–	–	0.0018	–4.726	–6.300	1.574
Li@C_{28}	1.453	2.442	1.27	0.0057	–3.725	–6.242	2.517
					–4.882	–6.468	1.586
Na@C_{28}	1.460	2.454	2.49	0.0025	–3.806	–6.298	2.492
					–4.926	–6.542	1.616
K@C_{28}	1.475	2.467	1.39	0.0017	–3.950	–6.418	2.468
					–4.998	–6.595	1.597
C_{28}^*	1.452	–	–	0.0013	–4.477	–6.054	1.577
Ti@C_{28}	1.470	2.547	0.20	2.1604	–3.517	–5.042	1.525
Zn@C_{28}	1.467	2.467	0.37	0.0034	–3.695	–6.203	2.508

Note: $d_{C\text{-}C}$ is the average bond length carbon−carbon in the fullerene framework, l is average distance from carbon atoms to embedded metal atom, Q_{ME} is charge on a metal atom, μ is the dipole moment, E_{LUMO} is the energy of the lower vacant molecular orbital, E_{HOMO} is the energy of the upper filled molecular orbital, ΔE_g is the width of the band gap; the entry C_{28}^* means that the data given for fullerene C_{28} were obtained by calculation using the cc-pVDZ base set, while the entry without an asterisk means that the data were obtained using 6-311++G(d,p).

dependence of the band gap width of fullerene C_{28} on the type of embedded atom is observed: initially, significantly increasing in the case of the atom Li, it slightly decreases (compared with Li@C_{28}) with the embedding of Na and K. The band gap of the considered fullerene slightly decreases when the Ti atom is embedded. When the Zn atom is embedded, the band gap significantly increases to 2.5 eV; the compound Zn@C_{28} has the strongest dielectric properties among all the compounds considered.

Now let's consider the impact of the fullerene size on the band gap width with the type of embedded atom unchanged (Fig. 2, *c*). It can be noted for all three cases under consideration, that the change of the considered value is more significant in case of the transition from 24 to 28 carbon atoms, and its increase is always observed. The change of the band gap is insignificant and has a different character for each case of transition from 20 to 24 carbon atoms. Considering Li-containing complexes, it can be established that the width of the band gap increases. The transition from 20 to 24 carbon atoms in case of Na-containing complexes has practically no effect on the band gap width, it can be assumed that its value remains unchanged. A decrease of the band gap is observed during the transition from 20 to 24 carbon atoms in the case of K-containing complexes.

Fig. 3 shows the constructed graphs of the density function of states and single-electron spectra. It should be noted that an unrestricted Hartree−Fock scheme was used for calculating complexes with alkali metals, the studied systems are systems with open shells. Electrons in alpha molecular orbitals with a spin-up state and beta molecular orbitals with a spin-down state were considered independently. In most cases, this did not affect the position of the Fermi level, the values obtained were close and with an independent calculation of the band gap width in both variants. However, we observe a significant difference (on the order of 1 eV) of the values of the band gap in the case of fullerene complexes C_{28} when using alpha and beta orbitals in calculations of energies. The data calculated using alpha orbitals were used to construct figures 2, *a, c*. For this reason, Fig. 3 does not show the Fermi level positions for fullerene complexes C_{28} with alkali metals.

The main characteristics considered for all studied systems are given in the table. For complexes C_{28} with alkali

metals, the first row of values E_{LUMO}, E_{HOMO} and ΔE_g refers to electrons in alpha orbitals, the second row of values refers to electrons in beta orbitals.

Conclusion

In the framework of the work, the geometric and electronic characteristics of endohedral complexes of small fullerenes with atoms of some alkali and transition metals were considered. The impact of intercalation by metal atoms on the size of a fullerene cage, depending on the ordinal number of the metal, was determined. The electron density distribution is estimated based on the analysis of the charge distribution. The dependence between the type of embedded atom and the band gap is determined, graphs of the density of states function and single-electron spectra for the considered structures are obtained.

The following was found a result of the conducted study:

• the introduction of metal atoms causes an increase of the average length of bond of carbon−carbon of the fullerene cage. The impact of metal atom on the geometric structure strengthens in case of alkali metals with an increase of the ordinal number of the metal. It is noted that the greater the number of carbon atoms in the fullerene cage, the weaker is the impact of metal atom on the geometric characteristics, compared with fullerenes with a smaller number of carbon atoms in the structure. A stronger impact of the embedded titanium atom on the geometry of the complex in comparison with zinc is observed in case of transition metals;

• the dependence of the charge on the alkali metal atom on its ordinal number is different for different fullerenes. If in the cases of fullerenes C_{20} and C_{24} the charge on the metal atom increased with increasing sequence number, then the maximum charge value for fullerene C_{28} was reached on the sodium atom. In complexes with transition metals, the zinc atom acquires a higher charge compared to the titanium atom in a complex with fullerene C_{28};

• the band gap width can be controlled by intercalating small fullerenes with metal atoms. Complexes of fullerenes C_{20} and C_{24} with alkali metals have a smaller band gap compared to the initial structure, and the larger the ordinal number of the metal atom, the lower the value of the considered parameter. There is an ambiguity of the dependence for the case of fullerene C_{28}, which requires further studies for resolving. The embedding of a zinc atom into fullerene C_{28} results in a significant increase of the band gap width, the resulting complex has the highest value of this parameter among all the structures considered in the work; the titanium atom slightly reduces the value of the band gap width.

The results obtained in this study can be useful for the development of new heterostructures for the needs of solar energy. This is attributable to the fact that possible ferroelectric properties of endohedral fullerenes, combined with large values of the dipole moment, which were determined for various structures in the work, determine their possible use in highly efficient photovoltaic elements. Heterostructures, the constituent elements of which are endohedral fullerenes, can also be useful for optical applications, for example, for designing devices based on two-dimensional photonic crystals, which is determined by the possibility of regulating the refractive index of the medium by changing the band gap by intercalating nanostructures with metals.

Funding

This study was carried out under state assignment of the Ministry of Science and Higher Education of the Russian Federation (project „FZUU-2023-0001“).

Conflict of interest

The authors declare that they have no conflict of interest.

References

[1] P.V. Pham, S.C. Bodepudi, K. Shehzad, Y. Liu, Y. Xu, B. Yu, X. Duan. Chem. Rev., **122** (6), 6514 (2022). DOI: 10.1021/acs.chemrev.1c00735
[2] D. Jena, K. Banerjee, G.H. Xing. Nat. Mater., **13** (12), 1076 (2014). DOI: 10.1038/nmat4121
[3] R. Sakthivel, M. Keerthi, R.J. Chung, J.H. He. Prog. Mater. Sci., **132**, 101024 (2023). DOI: 10.1016/j.pmatsci.2022.101024
[4] Y. Zhang, Y. Li, Q. You, J. Sun, K. Li, H. Hong, L. Kong, M. Zhu, T. Deng, Z. Liu. Nanoscale, **15** (3), 1402 (2023). DOI: 10.1039/D2NR05819G
[5] J. Hao, H. Lu, L. Mao, X. Chen, M.C. Beard, J.L. Blackburn. ACS Nano, **15** (4), 7608 (2021). DOI: 10.1021/acsnano.1c01134
[6] Lv. Qian, Lv. Ruitao. Carbon, **145**, 240 (2019). DOI: 10.1016/j.carbon.2019.01.008
[7] A.N. Gusev, A.S. Mazinov, A.S. Tyutyunik, V.S. Gurchenko. RENSIT, **11** (3), 331 (2019) (in Russian). DOI: 10.17725/rensit.2019.11.331
[8] A.V. Eletskii. Phys.-Usp., **43** (2), 111 (2000). DOI: 10.1070/PU2000v043n02ABEH000646
[9] L. Mengyang, Z. Ruisheng, D. Jingshuang, Z. Xiang. Coord. Chem. Rev., **471**, 214762 (2022). DOI: 10.1016/j.ccr.2022.214762
[10] Z.N. Cisneros-García, D.A. Herná ndez, F.J. Tenorio, J.L. Rodríguez-Zavala. Mol. Phys., **118** (14), e1705411 (2020). DOI: 10.1080/00268976.2019.1705411
[11] J.S. Nam, Y. Seo, J. Han, J.W. Lee, K. Kim, T. Rane, H.D. Kim, I. Jeon. Chem. Mater., **35** (20), 8323 (2023). DOI: 10.1021/acs.chemmater.3c01192
[12] X. Zhou, W. Zhang, S. Wang, F. Wen, Q. Chen, X. Shen, X. Hu, C. Peng, Z. Ma, M. Zhang, Y. Huang, S. Yang, W. Zhang. Sci. China Mater., **65**, 2325 (2022). DOI: 10.1007/s40843-021-1983-3
[13] M. Su, Y. Hu, S. Yang, A. Yu, P. Peng, L. Yang, P. Jin, B. Su, F.F. Li. Adv. Electron. Mater., **8** (1), 2100753 (2022). DOI: 10.1002/aelm.202100753
[14] M. Alshammari, T. Alotaibi, M. Alotaibi, A.K. Ismael. Energies, **16** (11), 4342 (2023). DOI: 10.3390/en16114342

[15] T. Wang, C. Wang. Small, **15** (48), 1901522 (2019). DOI: 10.1002/smll.201901522
[16] E.M. Shpilevsky, S.A. Filatov, A.G. Soldatov, G. Shilagardi. V sb. *Materialy i struktury sovremennoy elektroniki: Materialy X Mezhdunarodnoj nauchnoj konferencii*, edited by V.B. Odzhaev (main ed.), N.A. Poklonsky, V.A. Pilipenko, P. Zhukovsky, V.V. Petrov, M.G. Lukashevich, N.M. Lapchuk, V.S. Prosolovich, I.I. Azarko, N.I. Gorbachuk, S.A. Vyrko, T.M. Lapchuk, A.N. Oleshkevich (Belarusian State University, Minsk, 2022), p. 575 (in Russian).
[17] J. Li, L. Chen, L. Yan, Z. Gu, Z. Chen, A. Zhang, F. Zhao. Molecules, **24** (13), 2387 (2019). DOI: 10.3390/molecules24132387
[18] I.V. Mikheev, M.M. Sozarukova, D.Y. Izmailov, I.E. Kareev, E.V. Proskurnina, M.A. Proskurnin. Int. J. Mol. Sci., **22**, 5838 (2021). DOI: 10.3390/ijms22115838
[19] W.P. Kopcha, R. Biswas, Y. Sun, S.T.D. Chueng, H.C. Dorn, J. Zhang. Chem. Commun., **59**, 13551 (2023). DOI: 10.1039/D3CC03603K
[20] V.T. Lebedev, N.A. Charykov, O.S. Shemchuk, I.V. Murin, D.A. Nerukh, A.V. Petrov, D.N. Maystrenko, O.E. Molchanov, V.V. Sharoyko, K.N. Semenov. Colloids and Surfaces B: Biointerfaces, **222**, 113133 (2023). DOI: 10.1016/j.colsurfb.2023.113133
[21] A.N. Gusev, A.S. Mazinov, A.I. Shevchenko, A.S. Tyutyunik, V.S. Gurchenko, E.V. Braga. Prikladnaya fizika, **6**, 48 (2019) (in Russian).
[22] H.J. Zhou, D.H. Xu, O.H. Yang, X.Y. Liu, G. Gui, L. Li Dalton Trans., **50** (19), 6725 (2021).
[23] P. Zhang, T. Xue, Z. Wang, W. Wei, X. Xie, R. Jia, W. Li. Inorg. Chem. Front., **10**, 7238 (2023). DOI: 10.1039/D3QI01105D
[24] X.H. Cai, Q. Yang, M. Wang. Appl. Surf. Sci., **575**, 151660 (2022). DOI: 10.1016/j.apsusc.2021.151660
[25] J. Li, R. Wu. Appl. Phys. Lett., **120** (2), 023301 (2022). DOI: 10.1063/5.0076267
[26] B. Mortazavi, Y. Rémond, H. Fang, T. Rabczuk, X. Zhuang. Mater. Today Commun., **36**, 106856 (2023). DOI: 10.1016/j.mtcomm.2023.106856
[27] P.W. Dunk, N.K. Kaiser, M. Mulet-Gas, A. Rodríguez-Fortea, J.M. Poblet, H. Shinohara, C.L. Hendrickson, A.G. Marshall, H.W. Kroto. J. Am. Chem. Soc., **134** (22), 9380 (2012). DOI: 10.1021/ja302398h
[28] P.W. Dunk, M. Mulet-Gas, Y. Nakanishi, N.K. Kaiser, A. Rodríguez-Fortea, H. Shinohara, J.M. Poblet, A.G. Marshall, H.W. Kroto. Nat. Commun., **5**, 5844 (2014). DOI: 10.1038/ncomms6844
[29] J. Zhao, Q. Du, S. Zhou, V. Kumar. Chem. Rev., **120** (17), 9021 (2020). DOI: 10.1021/acs.chemrev.9b00651
[30] A.V. Silant'ev. Phys. Metals Metallogr., **119** (6), 511 (2018). DOI: 10.1134/S0031918X18060133
[31] A.V. Silant'ev. Russ. Phys. J. **62**, 925 (2019). DOI: 10.1007/s11182-019-01798-6
[32] A.V. Silant'ev. Phys. Metals Metallogr., **121**, 195 (2020). DOI: 10.1134/S0031918X20010160
[33] A.V. Silant'ev. Phys. Metals Metallogr., **121**, 501 (2020). DOI: 10.1134/S0031918X20060149
[34] A.V. Silant'ev. Phys. Metals Metallogr., **122**, 315 (2021). DOI: 10.1134/S0031918X21040098
[35] I.V. Zaporotskova, N.P. Boroznina, S.V. Boroznin, E.S. Drychkov, Y.V. Butenko, M.B. Belonenko. Bull. Russ. Acad. Sci. Phys., **86** (6), 673 (2022). DOI: 10.3103/S1062873822060314
[36] I.V. Zaporotskova, S.V. Boroznin, M.B. Belonenko, E.S. Drychkov, Y.V. Butenko. Bull. Russ. Acad. Sci. Phys., **86** (12), 1450 (2022). DOI: 10.3103/S1062873822120292
[37] S.V. Boroznin, I.V. Zaporotskova, P.A. Zaporotskov, N.P. Boroznina, M. Govindasami, L.V. Kozhitov, A.V. Popkova. Izvestiya vuz. Materialy elektronnoy tekhniki , **25** (2), 137 (2022). (in Russian). DOI: 10.17073/1609-3577-2022-2-137-145.
[38] W. Koch, M.C. Holthausen. *A Chemist's Guide to Density Functional Theory* (Wiley-VCH, Weinheim, 2001)
[39] P. Schwerdtfeger, L.N. Wirz, J. Avery. WIREs Comput. Mol. Sci., **5** (1), 96 (2015). DOI: 10.1002/wcms.1207
[40] V. Andova, F. Kardoš, R. Škrekovski. Ars Mathematica Contemporanea, **11**, 353 (2016).
[41] G.R. Schleder, A.C.M. Padilha, C.M. Acosta, M. Costa, A. Fazzio. J. Phys.: Mater., **2** (3), 032001 (2019). DOI: 10.1088/2515-7639/ab084b
[42] A.H. Mazurek, Ł. Szeleszczuk, D.M. Pisklak. Pharmaceutics, **12** (5), 415 (2020). DOI: 10.3390/pharmaceutics12050415
[43] Q. He, B. Yu, Z. Li, Y. Zhao. Energy Environ. Mater., **2** (4), 264 (2019). DOI: 10.1002/eem2.12056
[44] E. Napió rkowska, K. Milcarz, Ł. Szeleszczuk. Int. J. Mol. Sci., **24** (18), 14155 (2023). DOI: 10.3390/ijms241814155
[45] E.K. Sarikaya, Ö. Dereli, S. Bahçeli. Adiyaman Univ. J. Sci., **11**, 456 (2021). DOI: 10.37094/adyujsci.938050
[46] K. Soyarslan, B. Ortatepe, B. Yurduguzel, M.T. Güllüoğlu, Y. Erdogdu. J. Mol. Model., **28** (11), 352 (2022). DOI: 10.1007/s00894-022-05348-9
[47] E.R. Davidson, A.E. Clark. Int. J. Quantum Chem., **122** (8), e26860 (2022). DOI: 10.1002/qua.26860
[48] S.C. North, K.R. Jorgensen, J. Pricetolstoy, A.K. Wilson. Front. Chem., **11**, 1152500 (2023). DOI: 10.3389/fchem.2023.1152500
[49] N.M. O'Boyle, A.L. Tenderholt, K.M. Langner. J. Comp. Chem., **29**, 839 (2008). DOI: 10.1002/jcc.20823

Translated by A.Akhtyamov